UDK 669.1:620.173:621.78:539.92
Original scientific article/Izvirni znanstveni članek

ISSN 1580-2949
MTAEC9, 55(6)843(2021)

HIGH-TEMPERATURE DEFORMATION BEHAVIOR AND HOT-PROCESSING MAP OF 25CrMo4 AXLE STEEL BASED ON FRICTION CORRECTION

VISOKOTEMPERATURNA DEFORMACIJA IN NJENA PROCESNA MAPA NA OSNOVI KOREKCIJE TRENJA ZA JEKLO 25CrMo4

Keran Liu[1], Yuanming Huo[1,*], Tao He[1], Cunlong Huo[1], Changyuan Jia[1], Xiangyang Du[1], Baoyu Wang[2]

[1]School of Mechanical and Automotive Engineering, Shanghai University of Engineering Science, Shanghai 201620, China.
[2]School of Mechanical Engineering, University of Science and Technology Beijing, Beijing 100083, China

Prejem rokopisa – received: 2021-09-03; sprejem za objavo – accepted for publication: 2021-10-20

doi:10.17222/mit.2021.253

The deformation behavior and microstructure of 25CrMo4 axle steel was systematically investigated by thermal compression deformation. The hot-compression test of a 25CrMo4 axle steel sample was carried out on a Gleeble-3800 thermal mechanical simulation tester. The flow behavior of the alloy was studied at the deformation temperature (900–1200 °C), strain rates (0.01; 0.1; 1.0) s^{-1} and the maximum deformation of 60 %. The flow curves under different deformation conditions were obtained, and the effects of the deformation temperature and strain rate on the appearance of the flow curves are discussed. The true stress-strain curve obtained by experiment is modified by friction. Based on the corrected experimental data, the activation energy determined by the regression analysis was Q = 311 kJ/mol, and the constitutive model was constructed. The high-temperature flow behavior of the 25CrMo4 axle steel was described by the Zener-Hollomon parameter. The optimum hot-deformation process parameters were determined based on the hot processing maps, followed by the analysis of the microstructure characteristics of the alloys under optimum hot working. The results show that the suitable hot-deformation process parameters of the alloy are as follows: deformation temperature is 1050–1200 °C, and strain rate is 0.01 s^{-1} to 0.14 s^{-1}.

Keywords: 25CrMo4 axle steel, hot-compression test, hot processing map, friction correction

Avtorji so v članku preiskovali vročo tlačno deformacijo jekla za osi in gredi vrste 25CrMo4. Preizkusi so bili izvajani na preizkuševalniku za termično mehansko simulacijo Gleeble-3800. Preučevali so plastično tečenje izbranega jekla v območjih temperatur deformacije med 900 °C in 1200 °C, pri hitrostih deformacije 0,01s^{-1}, 0,1s^{-1} in 1,0 s^{-1} ter maksimalni 60 %-tni deformaciji. Pri izbranih pogojih deformacije je bila izdelana krivulja plastičnega tečenja, obravnavali pa so tudi vpliv izbranih pogojev deformacije. Dobljene eksperimentalne krivulje odvisnosti med pravo (resnično) napetostjo in pravo deformacijo (angl.: true stress-true strain) so modificirali z vplivom trenja. Na osnovi korigiranih eksperimentalnih podatkov so z regresijsko analizo določili aktivacijsko energijo Q = 311 kJ/mol in konstruirali konstitutivni model. Visokotemperaturno deformacijo jekla 25CrMo4 so opisali s Zener-Hollomonovim parametrom. Na osnovi procesne mape vroče deformacije so določili optimalne parametre vroče tlačne deformacije za izbrano jeklo. Sledila je analiza mikrostrukture pri optimalnih pogojih vroče deformacije. Rezultati raziskave so pokazali da je za izbrano jeklo najprimernejši procesni pogoj vroče deformacije: temperatura deformacije med 1050 °C in 1200 °C ter njena hitrost med 0,01 s^{-1} in 0,14 s^{-1}.

Ključne besede: jeklo za gredi in osi 25CrMo4, vroči tlačni preizkus, procesna mapa

1 INTRODUCTION

A railway is the artery of a national economy and the key to ensuring economic development in various regions.[1] Compared with other modes of transportation, a railway is less affected by weather. Because of its frequent transportation and low cost, railway occupies a greater advantage in the transportation industry. As an important part of high-speed trains, axles realize the functions of bearing, guiding and braking in vehicle operation. Because of the complex working conditions and poor application environment, its performance and manufacturing quality are directly related to the safety and reliability of train operation.[2,3] High speeds and heavy loads are the main characteristics of high-speed railway axle working environment, so axle steel needs to have good toughness, high strength and hardenability to ensure its fatigue strength and service life. A study of the influence of deformation temperature and deformation rate on the mechanical behavior and microstructure evolution of 25CrMo4 axle steel provides valuable reference for the optimization of axle performance and quality.

At present, the research on 25CrMo4 axle steel mainly focuses on the influence of the heat treatment process on the microstructure and mechanical properties of the material, and there are also some reports on its mechanical behavior and microstructure evolution. Huo et al.[4] studied the hot-compression deformation behavior and microstructure evolution of 25CrMo4 steel at 1040–1160 °C. Zhou et al. studied the dynamic recrystallization behavior of 25CrMo4 steel, determined the dynamic recrystallization model and established the pro-

*Corresponding author's e-mail:
yuanming.huo@sues.edu.cn (Yuanming Huo)

Table 1: Chemical composition of 25CrMo4 axle steel (*w*/%)

C	Si	Mn	Cr	P	S	Ni	Cu	Mo	Fe
0.20	0.22	0.65	0.94	0.024	0.005	0.03	0.09	0.17	balance

cessing map.[5,6] Jiang et al.[7] studied the hot-compression deformation behavior of 25CrMo4 steel at strain rates of 0.1–10.0 s^{-1}, deformation temperatures of (1050; 1100; 1150) °C, and established the peak stress constitutive Equation of 25CrMo4 steel. In the process of plastic deformation, the flow stress of the material determines the load and energy required for processing.[8] The constitutive model reflects the relationship between the stress temperature, and strain rate. It is an essential model in the calculation and simulation of high-temperature deformation processes. It can be used to describe the flow behavior of materials in the process of hot deformation. Arrhenius model,[9] Johnson-Cook,[10] Zerilli-Armstrong[11] and Norton-Hoff model[12] are commonly used to describe the flow stress constitutive Equation of metallic materials at high temperatures. With the improvement of workpiece precision requirements, optimizing the hot-processing parameters is one of the main means to accurately control the microstructure and mechanical properties. At the same time, the flow stress of the material will be affected by the deformation degree, deformation temperature, deformation rate, friction force and temperature-rise effect.[13] In order to obtain an accurate mathematical model and processing map, the original experimental data need to be corrected. Wu et al.[14] corrected the flow stress curve of SA508-3 steel at temperatures of 800–1200 °C and a strain rate of 0.001 s^{-1} by friction. The corrected true-stress value is always less than the experimental value. The stress obtained from the experiment cannot correctly represent the real stress of the material, so it is necessary to correct the friction of the experimental data.

The aim of this work is to study the deformation behaviour and microstructure evolution of 25CrMo4 axle steel at the high temperature. Firstly, hot-compression tests were conducted with different process parameters to obtain the stress-strain relationship of 25CrMo4 axle steel. Secondly, we corrected the stress-strain data by friction, and established the constitutive Equation and hot processing map of the alloy. Thirdly, the effects of deformation temperature and strain rate on the mechanical behavior and microstructure evolution of 25CrMo4 axle steel were studied, and the suitable hot-processing parameters of the alloy were obtained.

2 EXPERIMENTAL PART

The material used in this paper is 25CrMo4 hot-rolled round steel bar (ϕ 12 mm) purchased from a steel plant. The chemical composition is shown in **Table 1**.

Before hot compression, the alloy bar was cut into a cylinder of ϕ 10 mm × 15 mm by wire cutting. The hot compression test was carried out on Gleeble-3800 thermal mechanical simulation tester. The test equipment is shown in **Figure 1**.

The deformation temperatures were (900; 950; 1000; 1050; 1100; 1150; 1200) °C, and the strain rates were 0.01 s^{-1}, 0.1 s^{-1} and 1.0 s^{-1}. The compression deformation of the sample was set to 60 %. The temperature of the sample is precisely controlled by a thermocouple. The thermocouple is welded in the middle of the sample with a spacing of 1–2 mm. The sample was heated to 1200 °C at a heating rate of 10 °C/s and kept for 3 min. Then the sample was cooled to the test temperature (900; 950; 1000; 1050; 1100; 1150; 1200) °C at a cooling rate of 10 °C/s for the compression test.[15] The hot-compression process of 25CrMo4 axle steel is shown in **Figure 2**. After the compression is completed, the sample is quenched by water immediately to retain the microstructure of the sample after hot compression. The data are automatically collected and saved by computer.

Figure 1: Gleeble-3800 thermal simulator machine

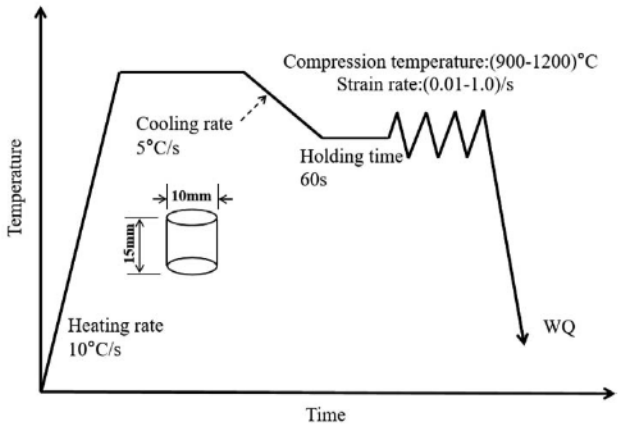

Figure 2: The hot-compression process of 25CrMo4 axle steel

In the hot compression test, the 'waist drum' phenomenon[16] easily occurs because the upper and lower ends of the sample inevitably produce friction in the machine contact. The validity of the experimental data is usually verified by the expansion coefficient B[17]. When $B \geq 0.9$, the data is considered to be valid. The calculation formula is as follows:

$$B = \frac{L_0 d_0^2}{L_1 d_1^2} \quad (1)$$

In Equation (1), B is the expansion coefficient; L_0 is the original length of the sample; d_0 is the original diameter of the sample; L_1 is the average length of the compressed sample; d_1 is the mean diameter of the compressed sample.

Through measurement and calculation, the expansion coefficient B is 1.09, indicating that the test results are effective. The compressed sample was cut along the diameter by a wire-cutting machine. In order to facilitate the subsequent operation, and the sample is setted by the hot-pressing inlay method. Rough grinding, fine grinding, polishing and corrosion of sample cross section. Corrosion solution using 60 mL pure water, 0.1 mL H_2O_2, 2.5 saturated picric acid solution, 0.2 g $C_{18}H_{29}NaO_3S$.

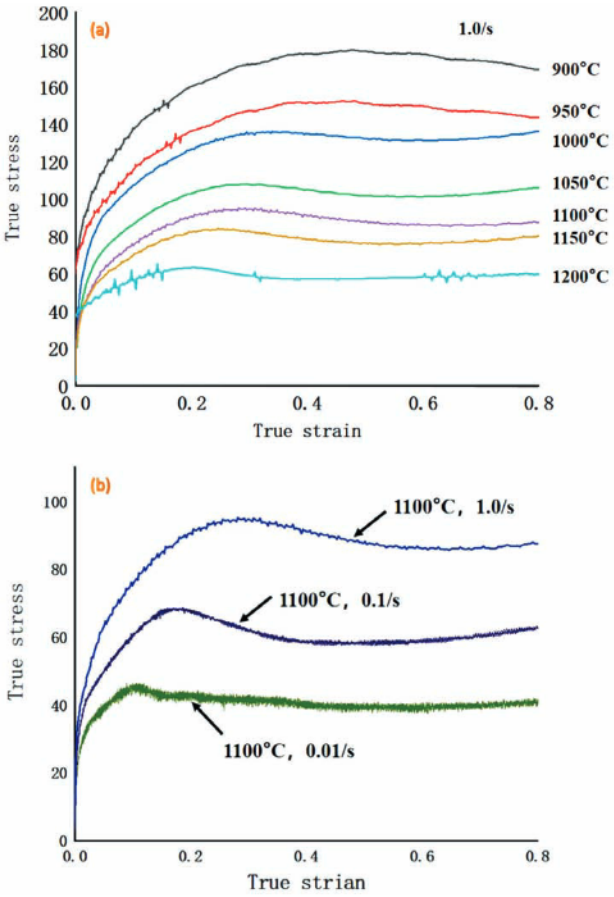

Figure 3: Experimental flow curves under different deformation conditions

Place the prepared corrosive solution in the 50 °C constant-temperature water bath for heating and storage.[4] After soaking the polished surface in the corrosive solution for about 1 min, remove the sample immediately and rinse the polished surface with pure water, and then wiped with alcohol cotton ball and dried. Finally, the grain morphology was observed by optical microscope and the microstructure photos were obtained.

3 RESULTS AND DISCUSSION

3.1 Characteristic analysis of flow stress curve

The flow-stress curve can reflect the deformation characteristics of the material in the plastic-deformation process. The flow stress curves of the 25CrMo4 axle steel at different deformation temperatures and strain rates are obtained in the experiment, as shown in **Figure 3.**

The curves under different deformation conditions show similar changes, and the true stress value is positively correlated with the deformation at the initial stage of deformation. When the peak stress is reached, with the increase of deformation, the true stress decreases to a certain stress value and tends to be stable, and the stress curve presents typical dynamic recrystallization characteristics.[18]

It can be seen from **Figure 3a** that at the same strain rate and different deformation temperatures, the higher the temperature, the shorter the time when the stress reaches the peak value, the smaller the peak stress, and the smaller the stress value at stable state. On the one hand, it may be that higher deformation temperature is beneficial to the early occurrence of dynamic recovery during the work-hardening stage. On the other hand, a higher deformation temperature makes recrystallization occur in a smaller deformation. At the same time, the work hardening against with the softening effect of dynamic recovery and recrystallization, so that makes the stress value smaller in a stable period.[17]

3.2 Friction correction of flow-stress curve based on Ebrahimi R Criterion

In the compression process, the friction between the sample and the discharge head will hinder the metal flow at the end face of the sample, change the stress state of the sample, and make the stress of the sample higher than the ideal state. Therefore, it is necessary to correct the true stress-strain curve by friction.[14] Ebrahimi et al.[19] proposed a friction-correction formula, in this paper, the curve is corrected by Equation (2).[20]

$$P_1 = \frac{P_0 C^2}{(2e^C - C - 1)} \quad (2)$$

In Equation (2), P_0 is the flow stress before correction, P_1 is the flow stress after correction. The instanta-

neous correction constant C is expressed by Equation (3):

$$C = \frac{2\mu R}{h} \tag{3}$$

$$R = R_0\sqrt{\frac{h_0}{h}} \tag{4}$$

In Equation (3), R is the instantaneous radius of the sample, μ is a friction factor. In Equation (4), R_0 is the initial radius of the sample, h is the instantaneous height of the sample and h_0 is the initial height of the sample.

$$\mu = \frac{\frac{R_1}{h_1}b}{\frac{4}{\sqrt{3}} - \frac{2b}{3\sqrt{3}}} \tag{5}$$

$$R_1 = R_0\sqrt{\frac{h_0}{h_1}} \tag{6}$$

In Equation (6), R_1 is the average radius of the deformed sample; h_1 is the height of after deformed sample.

$$b = 4\frac{\Delta R}{R_1}\cdot\frac{h_1}{\Delta h_1} \tag{7}$$

$$\Delta h_1 = h_0 - h_1 \tag{8}$$

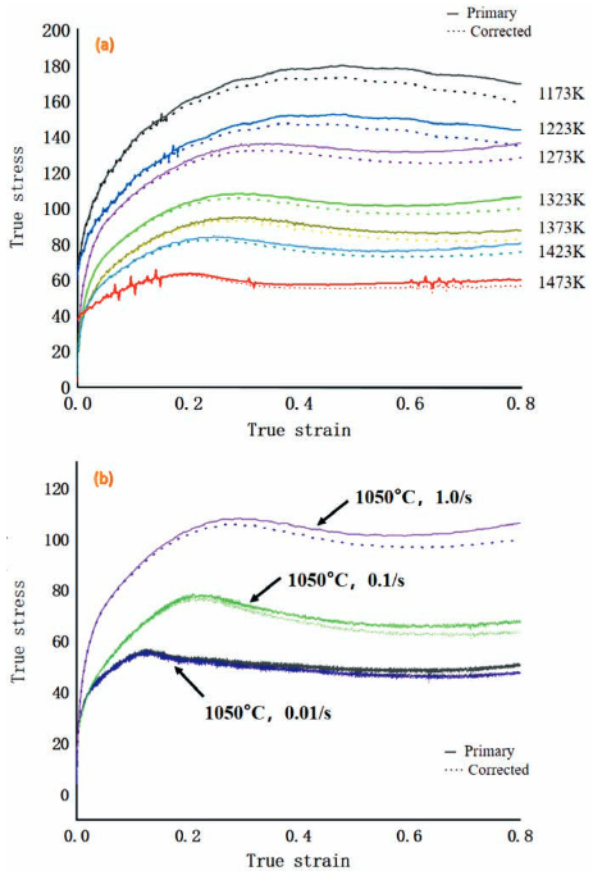

Figure 4: Flow-stress curves before and after correction

In Equation (7), Δh_1 is the compression variable; ΔR is the difference between the maximum bulging radius and the bottom radius of the sample, and the average value is measured repeatedly to reduce the measurement error.

The stress-strain curve of 25CrMo4 axle steel after friction modification is shown in **Figure 4.** The change trend of the flow stress curve before and after the friction modification is consistent, and the modified stress value is always less than the measured value. With the increase of the strain, stress deviation increases gradually before and after modification, which indicates that the influence of friction on the flow stress curve increases gradually. The reason may be that the inhomogeneity caused by friction during compression is proportional to the strain variable. At the beginning of compression, the deviation between the corrected curve and the measured flow stress curve is small. With the continuous increase of deformation, the drum deformation of the sample become large, and the contact area made large.[14] The effect of friction on flow stress increases gradually and the deviation between the corrected value and the measured value gradually increases. It can be found from **Figure 4** that even if the lubrication effect is good in the experiment, the bulge of the sample after machining is small, and the friction still has a certain influence on the flow stress. The importance of using tantalum sheet in a high-temperature compression experiment and friction correction of the curve after the experiment is further explained.

3.3 Construction of constitutive Equation

Under high-temperature deformation, the Arrhenius Equation[9] is widely used to describe the relationship among flow stress, deformation temperature and strain rate.[21,22]

$$\dot{\varepsilon} = Af(\sigma)e^{-\frac{Q}{RT}} \tag{9}$$

In Equation (9), $\dot{\varepsilon}$ is the strain rate, T is the absolute temperature, R is the gas constant, R = 8.314 J/(K·mol), Q is the activation energy for hot deformation.

$$f(\sigma) = \begin{cases} \sigma^n \alpha\sigma < 0.8 \\ \exp(\beta\sigma)\alpha\sigma > 1.2 \\ [\sinh(\alpha\sigma)] \text{ for all } \sigma \end{cases} \tag{10}$$

In Equation (10), n, α, β are material constants. Under all stress states, Equation (9) can be expressed as:

$$\dot{\varepsilon} = [\sinh(\alpha\sigma)]^n e^{-\frac{Q}{RT}} \tag{11}$$

In Equation (11), A is a material constant. The effect of deformation temperature and strain rate on deformation behavior can be described by Zener-Holloman:[24]

$$Z = \dot{\varepsilon}e^{-\frac{Q}{RT}} = A[\sinh(\alpha\sigma)]^n \tag{12}$$

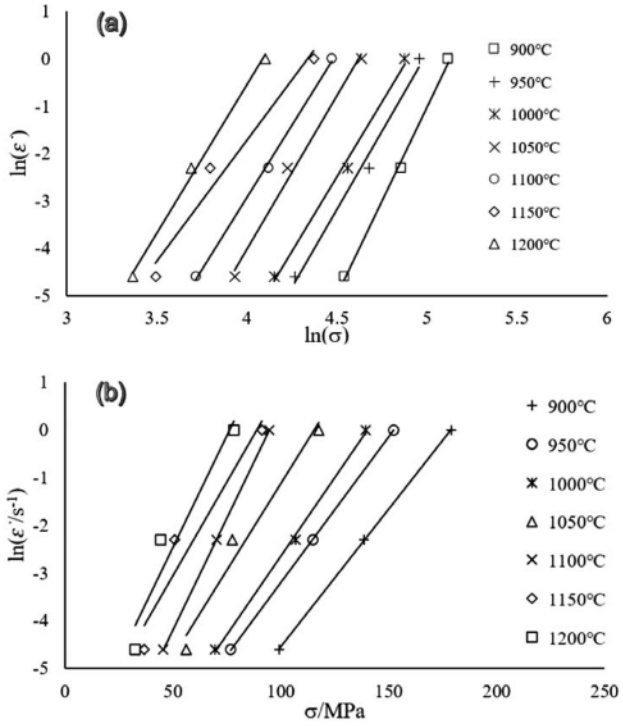

Figure 5: Relationship between flow stress and strain rate for 25CrMo4 axle steel at different temperatures

When the deformation temperature or strain rate is constant, the linear regression diagrams between the logarithm of flow stress and strain rate (ln σ – ln $\dot{\varepsilon}$, ln (sinh($\alpha\cdot\sigma$)) – ln $\dot{\varepsilon}$), flow stress and the logarithm of strain rate (σ– ln $\dot{\varepsilon}$), the logarithm of flow stress and the reciprocal of absolute temperature (ln ($\alpha\cdot\sigma$)– 1/T), the logarithm of flow stress and the logarithm of Z (ln ($\alpha\cdot\sigma$)– ln Z) are shown on **Figures 5** to **8**.

The required constants of the constitutive Equation can be obtained from the average slope of the straight line in **Figures 5** to **8**. Calculated: $A = 3.18 \times 10^{11}$ s^{-1}, $\alpha = 0.011689$ MPa^{-1}, $n = 4.8975$, $Q = 311.1914$ kJ/mol. In **Figure 8**, the correlation coefficient reaches 0.9884, which demonstrates the high accuracy of the material constants for describing the flow stress.

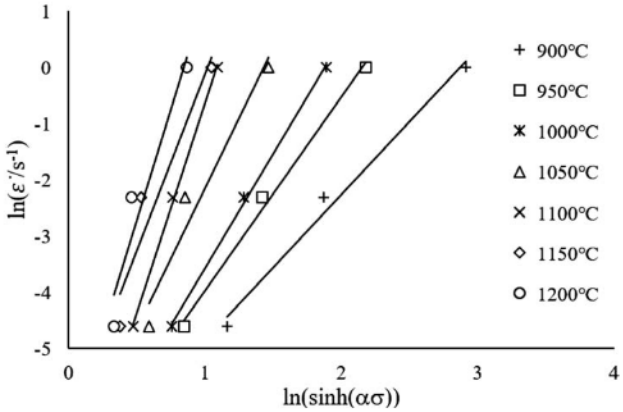

Figure 6: Relationship curves of ln (sinh($\alpha\cdot\sigma$)) – ln $\dot{\varepsilon}$) for 25CrMo4 axle steel at different temperatures

3.4 Determination of optimum process parameters for 25CrMo4 axle steel based on hot-processing map

3.4.1 Establishment of hot-processing map

The hot-processing map is mainly based on the dynamic material model theory, it reflects the suitable processing conditions of materials under different deformation conditions. According to the law of conservation of energy, the energy consumption in machining process can be written as:[23]

$$P = G + J \tag{13}$$

In Equation (13), P is the total energy for the external input to the material. G is a dissipative energy, which is the energy consumed by the plastic deformation of materials under an external force. J is the dissipation coefficient, which is the energy consumed by certain changes in grain structure during the thermal deformation of materials.

The instantaneous power P consumed per unit volume of material can also be expressed as the product of strain rate and flow stress, and Equation (13) can be written as:

$$P = \sigma\dot{\varepsilon} = G + J = \int_0^{\dot{\varepsilon}} \sigma \mathrm{d}\dot{\varepsilon} + \int_0^{\sigma} \dot{\varepsilon} \mathrm{d}\sigma \tag{14}$$

In the thermal deformation process, when the temperature and strain are constant, the flow stress can be ex-

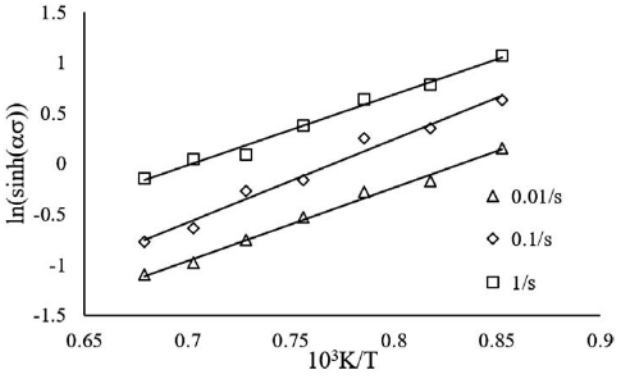

Figure 7: Relationship between flow stress and deformation temperatures of 25CrMo4 axle steel

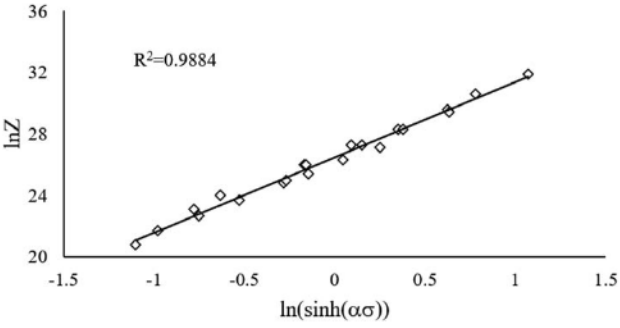

Figure 8: Relationship between flow stress and Zener-Hollomon parameter

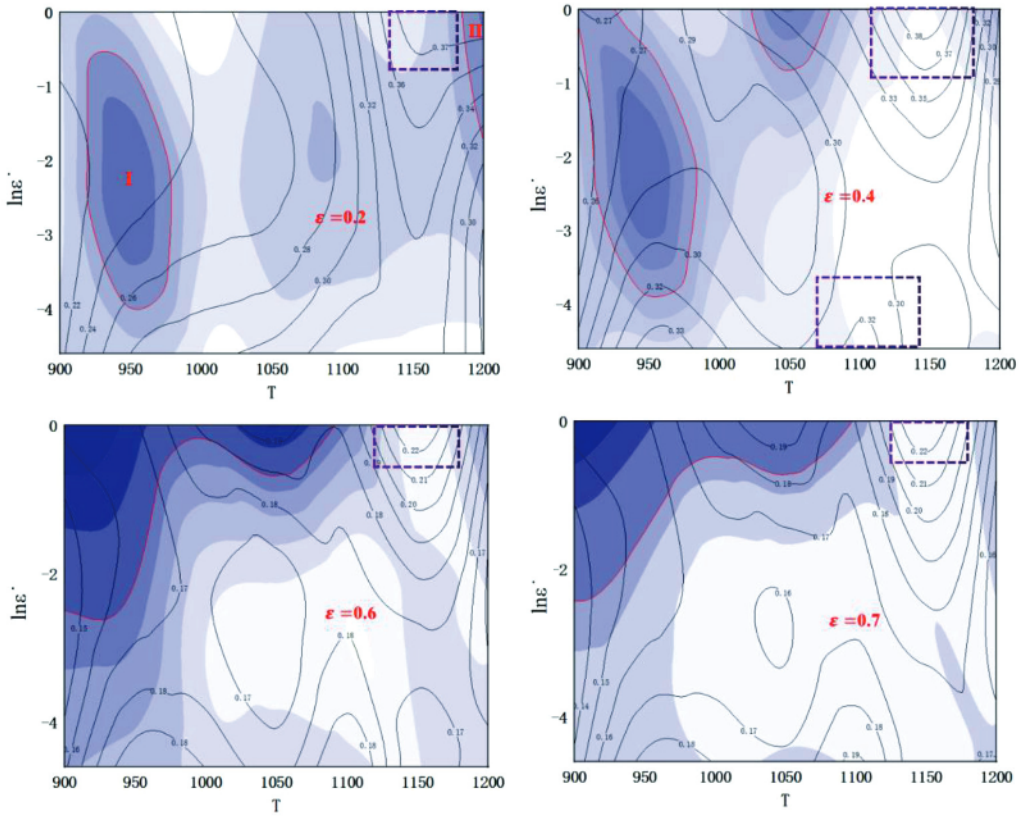

Figure 9: The hot-processing map for strains 0.2, 0.4, 0.6 and 0.7

pressed as $\sigma = K\dot{\varepsilon}^m$, where K is a constant, and m is the strain rate sensitivity index.

$$m = \frac{\mathrm{d}J}{\mathrm{d}G} = \left[\frac{\partial \ln \sigma}{\partial \dot{\varepsilon}}\right]_{\varepsilon,T} \tag{15}$$

In the nonlinear dissipation process, the ratio of the energy consumed by the evolution of microstructure during thermal deformation to the total energy consumed during thermal deformation can be expressed by a dimensionless parameter η:

$$\eta = \frac{J}{J_{\max}} = \frac{2m}{1+m} \tag{16}$$

The Kumar-Prasad instability criterion[24,25] derived from the principle of irreversible mechanical extremum can be expressed as:

$$\xi(\dot{\varepsilon}) = \frac{\partial \ln\left(\frac{m}{m+1}\right)}{\partial \ln \dot{\varepsilon}} + m < 0 \tag{17}$$

In Equation (17), ξ is the instability factor, and the region with $\xi(\dot{\varepsilon}) < 0$ is the instability region.

3.4.2 Analysis of the hot-processing map and microstructure evolution

The friction correction data are extended by cubic spline interpolation method, and the hot processing maps are drawn when the strain is 0.2, 0.4, 0.6 and 0.7, respectively.

As shown in **Figure 9**, the value on the contour is the power dissipation efficiency (that is the value of η), which reflects the change rate of the microstructure during the hot-working deformation of materials. When the value of η is higher, the tissue transformation is more stable. The shadow part is the superimposed instability diagram, and the selected area of red solid line box represents the "unsafe" area with instability parameter less than zero, which should be avoided in the actual thermal processing. It can be seen from **Figure 9** that when the strain is 0.4, the instability region contour is similar to that when the strain is 0.2, but the area of the “unsafe” region is large. When the strain is 0.6 and 0.7, the contour of the instability region is similar.

A low-deformation temperature cannot provide the driving force for dynamic recrystallization, resulting in coarse grains. Too high a deformation temperature inhibits the occurrence of dynamic recrystallization. Under the same deformation, the deformation time is positively correlated with the strain rate. The deformation time is shortened, and the grain cannot be changed, which is also not suitable for workpiece processing. From the hot processing map, we can see that the unstable region is mainly concentrated in the left side of the hot-processing map, that is the high-temperature and high-strain-rate region and the low-deformation temperature region.

It will appear as two instability regions when the strain is 0.2. In the instability region I, the deformation

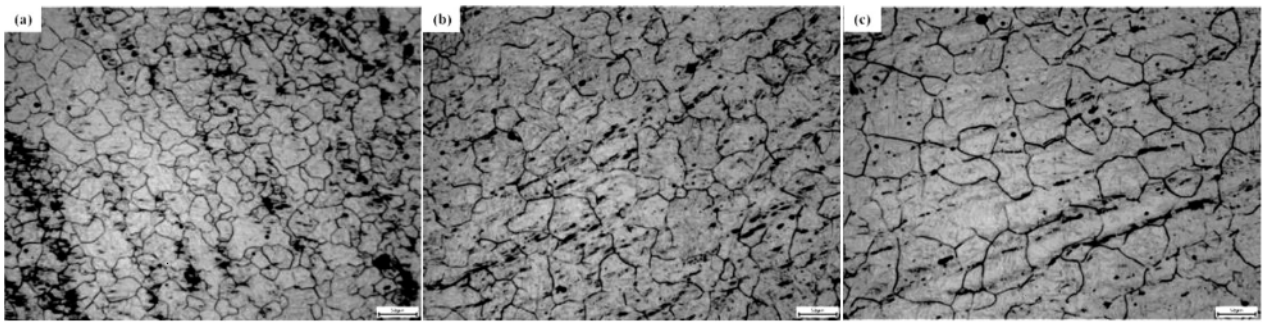

Figure 10: Microstructure of 25CrMo4 deformed at: a) T = 1050 °C, $\dot{\varepsilon}$ = 0.1 s^{-1}, b) T = 1100 °C, $\dot{\varepsilon}$ =0.1 s^{-1}, c) T = 1150 °C, $\dot{\varepsilon}$ = 0.1 s^{-1}

temperature is low, resulting in less energy to change the microstructure of the material, and the alloy is likely to produce adiabatic shear band due to thermal viscoplastic instability. In the instability region II, under high temperature and high strain rate, the material easily becomes unstable due to the local flow caused by the stress concentration by heat and interface slip.[26] In the low-strain-rate region with strain rate of 0.01 s^{-1} and the temperature of 1075–1175 °C, the maximum power dissipation value reaches 0.33, which is the processing safety region.

In general, the material instability refers to the adiabatic shear or local rheological instability of the material in the deformation process, and the instability in the actual production process is not suitable for the machining of the workpiece. In addition to the instability region, there is no region where the power-dissipation factor decreases sharply with the decrease of the strain rate. Although with the increase of strain, the mean value of the power-dissipation factor decreases slowly, and the proportion of dissipation energy in the tissue evolution decreases, all belong to the safe processing region, which can be selected according to the actual processing requirements. The power dissipation factor in the purple dashed line shows a gradual increase, which is the most suitable deformation region selected in this paper, and it is the best processing region.

The microstructures of the samples in the optimal processing area, 1050 °C–0.1 s^{-1}, 1100 °C–0.1 s^{-1} and 1150 °C–0.1 s^{-1}, are shown in **Figure 10**.

Figures 10a to **10c** show the micrographs of 25CrMo4 axle steel with forming temperatures of (1050; 1100; 1150) °C, respectively. It is obvious that the average grain size increases with the increase of the deformation temperature. The average grain sizes were measured as 23.53 μm, 36.7 μm and 48.78 μm. It can be seen from **Figure 10** that the grain morphology of 25CrMo4 axle steel is mostly uniform equiaxed grains, the microstructures of these samples exhibit wavy grain boundaries, which are indicative of a dynamic recrystallization process. These results match with the predictions of the processing map, so 25CrMo4 axle steel is suitable for hot processing in this region. Among them, the small black spots in the grain boundaries are carbide particles that are not completely dissolved and diffused in the austenitizing process. With the increase of the strain rate, the number of residual unmelted carbides decreases gradually, and the width and number of deformation bands decrease obviously.

4 CONCLUSIONS

On the Gleeble-3800 thermal simulation test machine, the hot-compression tests of axle steel were carried out at the strain rates of 0.01 s^{-1}, 0.1 s^{-1}, 1.0 s^{-1} and the deformation temperatures of (900; 950; 1000; 1050; 1100; 1150; 1200) °C, and the stress-strain curves of 25CrMo4 axle steel were obtained. The flow-stress curves are similar under different deformation conditions, and have obvious dynamic recrystallization characteristics. In the initial stage of deformation, the true stress increases rapidly with the increase of strain. When the true strain reaches a certain value, the curve reaches the peak. With the continuous increase of deformation degree, dynamic recrystallization occurs, and the material softens, and the true strain decreases.

The results of friction correction of flow stress data show that the change trend of the curve before and after friction correction is consistent, and the corrected stress value is always less than the measured value. With the increase of strain, the difference of true-stress value before and after modification increases gradually, and the influence of friction on the flow-stress curve increases gradually. The deviation between the corrected value and the measured value increases gradually.

Based on the dynamic material model, the hot-processing map of the 25CrMo4 axle steel is established by using the true stress-strain curve corrected by friction. It is found that there are two unstable regions in the processing map of 25CrMo4 axle steel when the strain is 0.2. The unstable region is mainly concentrated on the left side of the processing map, that is the high-temperature and high-strain-rate region and the low-deformation-temperature region. The suitable hot-deformation process parameters of the 25CrMo4 axle steel are obtained: deformation temperature is 1050–1200°C, strain rate is 0.01 s^{-1} to 0.14 s^{-1}.

Acknowledgments

This project is funded by the National Key Research and Development Program of China (Grant No. 2018YFB1307900), National Natural Science Foundation of China (Grant No. 51805314), Shanghai Science and Technology Commission (Grant No. 16030501200).

5 REFERENCES

[1] X. R. Meng, Study on Operation Mode of High Speed Express, IOP Conference Series: Earth and Environmental Science, 546 (**2020**) 5, doi:10.1088/1755-1315/546/5/052033

[2] S. J. Wang, J. Han, W. Zeng, X. M. Zhang, J. W. Zhao, G. Z. Dai, Effect of Low Temperature on Mechanical Properties of ER8 Steel for Wheel Rim, Chinese Journal of Materials Research, 32 (**2018**), 401–408, doi:CNKI:SUN:CYJB.0.2018-06-001

[3] J. Y. Liu, X. G. Liu, X. F. Qin, Research and Application of Axle Technology for Heavy Axle Railway Freight Cars, Rolling Stock, 52 (**2014**) 7, 1–5, doi:CNKI:SUN:TDCL.0.2014-07-001.

[4] Y. M. Huo, B. Y. Wang, J. G. Lin, Q. Bai, H. C. Ji, X. F. Tang, Hot Compression Deformation Behavior and Microstructure Evolution Rule of a High-Speed Railway Axle Steel, Indian Journal of Engineering & Materials Sciences, 24 (**2017**) 6, 447–454

[5] P. Zhou, Q. X. Ma, Static recrystallization behavior of 25CrMo4 mirror plate steel during two-pass hot deformation, Journal of Iron and Steel Research International 24 (**2017**) 2, doi:10.1016s-11006-706X(17)30031-6

[6] P. Zhou, Q. X. Ma, Dynamic Recrystallization Behavior and Processing Map Development of 25CrMo4 Mirror Plate Steel During Hot Deformation, Acta Metallurgica Sinica (English Letters), 30 (**2017**) 9, 907–920, doi:CNKI:SUN:JSXY.0.2017-09-012

[7] Y. Jing, B. Y. Wang, Y. M. Huo, X. Xiao, Thermal compressive deformation behavior and flow stress constitutive Equation of 25CrMo4 steel, Journal of Plasticity Engineering, 27 (**2020**) 5, 167–173, doi:10. 3969 /j. issn. 1007-2012. 2020. 05. 021

[8] H. Z. Li, X. M. Zhang, M. A. Chen, Z. P. Zhou, Hot deformation behavior of 2519 aluminum alloy, The Chinese Journal of Nonferrous Metals, 4 (**2005**), 621–625, doi:10.19476/j.ysxb.1004.0609.2005.04.021

[9] J. Cai, F. G. Li, T. Y. Liu, B. Chen, M. He, Constitutive Equations for elevated temperature flow stress of Ti-6Al-4V alloy considering the effect of strain, Materials and Design, 32 (**2010**) 3, doi:10.1016/j.matdes.2010.11.004

[10] Y. H. Zhao, J. Sun, J. F. Li, Y. Q. Yan, P. Wang, A comparative study on Johnson-Cook and modified Johnson-Cook constitutive material model to predict the dynamic behavior laser additive manufacturing FeCr alloy, Journal of Alloys and Compounds, 723 (**2017**), doi:10.1016/j.jallcom.2017.06.251

[11] Y. C. Lin, X. M. Chen, A combined Johnson-Cook and Zerilli-Armstrong model for hot compressed typical high-strength alloy steel, Computational materials science, 50 (**2010**) 10, doi:10.1016/j.commatsci.2010.09.001

[12] M. Milesi, R. E. Logé, D. Pino Muñoz, Y. Jansen, P.-O. Bouchard, Accounting for material parameters scattering in rolled zinc formability, Journal of Materials Processing Tech., 245 (**2017**), 134–148, doi:10.1016/j.jmatprotec.2017.02.021

[13] W. L. Gao, Y. F. Guan, Correction of flow stress-strain curve and processing maps of 5083 aluminum alloy during hot compression, The Chinese Journal of Nonferrous Metals, 28 (**2018**) 9, 1737–1745, doi:10.19476/j.ysxb.1004.0609.2018.09.04

[14] J. G. Wu, H. P. An, L. L. Liu, Q. S. Li, High-temperature constitutive Equation of SA508-3 steel based on friction correction, Forging & stamping technology, 45 (**2020**) 12, 178–182, doi:10.13330/j.issn.1000-3940.2020.12.030

[15] J. Hu, P. Du, D. F. Li, S. L. Guo, X. Q. Xu, X. P. Wu, Flow stress behavior of Zn-Cu-Cr alloy during hot compression deformation, Journal of plasticity engineering, 18 (**2011**) 1, 101–106, doi:CNKI:SUN:SXGC.0.2011-01-024

[16] Y. Gong, F. Zheng, S. H. Jiao, Positioning the metallographic observation site in a cylinder compression sample for the thermal simulation, PTCA (Part A: physical testing), 6 (**2004**), 282–285, doi:CNKI:SUN:LHJW.0.2004-06-005

[17] M. Gao, X. Zhao, J. Liu, B. X. Zhang, Z. M. Zhang, Research on hot deformation constitutive Equation and hot processing map of new-type Al-Zn-Mg-Cu alloy with high strength and ductility, Journal of plasticity engineering, 28 (**2021**) 3, 126–136, doi:10.3969/j.issn. 1007-2012. 2021. 03. 017

[18] X. H. Zhang, Y. Q. Bai, X. B. Jia, Hot deformation behavior and high temperature plastic constitutive Equation of LZ50 steel for axle, Heat treatment of metals, 45 (**2020**) 10, 31–34, doi:10.13251/j.issn.0254-6051.2020.10.006

[19] R. Ebrahimi, A. Najafizadeh, A new method for evaluation of friction in bulk metal forming, Journal of Materials Processing Tech., 152 (**2004**) 2, doi:10.1016/j.jmatprotec.2004.03.029

[20] P. Wanjara, M. Jahazi, H. Monajati, S. Yue, J. P. Immarigeon, Hot working behavior of near-α alloy IMI834, Materials Science & Engineering A, 396 (**2005**) 1–2, 50–60, doi:org/10.1016/j.msea.2004.12.005

[21] H. J. McQueen, S. Yue, N. D. Ryan, E. Fry, Hot working characteristics of steels in austenitic state, Journal of Materials Processing Tech., 531(**1995**) 1, doi:10.1016/0924-0136(95)01987-P

[22] H. J. McQueen, E. Fry, J. Belling, Comparative constitutive constants for hot working of Al-4.4Mg-0.7Mn (AA5083), Journal of Materials Engineering and Performance, 10 (**2001**) 2, doi:10.1361/105994901770345178

[23] T. Seshacharyulu, S. C. Medeiros, W. G. Frazier, Y. V. R. K. Prasad, Microstructural mechanisms during hot working of commercial grade Ti-6Al-4V with lamellar starting structure, Materials Science & Engineering, 325 (**2002**) 1–2, doi:10.1016s-10921-5093(01)01448-4

[24] Y. V. R. K. Prasad, H. L.Gegel, S. M. Doraivelu, J. C. Malas, J. T. Morgan, K. A. Lark, D. R. Barker, Modeling of dynamic material behavior in hot deformation: Forging of Ti-6242, Metallurgical Transactions A, 15 (**1984**) 10, doi:10.1007/BF02664902

[25] T. Seshacharyulu, S. C. Medeiros, W. G. Frazier, Y. V. R. K. Prasad, Microstructural mechanisms during hot working of commercial grade Ti-6Al-4V with lamellar starting structure, Materials Science & Engineering A, 325 (**2002**) 1–2, doi:10.1016s-10921-5093(01)01448-4

[26] Q. S. Dai, X. Liu, P. Fu, J. Q. Zhang, Y. L. Deng, High-temperature deformation behavior and processing map of 5083 aluminum alloy, Journal of Central South University (Science and Technology), 48 (**2017**) 8, 1988–1994, doi:CNKI:SUN:ZNGD.0.2017-08-005